

PITHA 02/05
 CERN-TH/2002-019
 BUTP-02/2
 FERMILAB-Pub-02/016-T
 hep-ph/0202106
 February 2002

The $B^+ - B_d^0$ Lifetime Difference Beyond Leading Logarithms

MARTIN BENEKE¹, GERHARD BUCHALLA², CHRISTOPH GREUB³,
 ALEXANDER LENZ⁴ AND ULRICH NIERSTE^{2,5}

¹ *Institut für Theoretische Physik E, RWTH Aachen, Sommerfeldstraße 28,
 D-52074 Aachen, Germany.*

² *Theory Division, CERN, CH-1211 Geneva 23, Switzerland.*

³ *Institut für Theoretische Physik, Universität Bern, Sidlerstrasse 5,
 CH-3012 Berne, Switzerland.*

⁴ *Fakultät für Physik, Universität Regensburg, D-93040 Regensburg, Germany.*

⁵ *Fermi National Accelerator Laboratory, Batavia, IL 60510-500, USA.*

Abstract

We compute perturbative QCD corrections to the lifetime splitting between the charged and neutral B meson in the framework of the heavy quark expansion. These next-to-leading logarithmic corrections are necessary for a meaningful use of hadronic matrix elements of local operators from lattice gauge theory. We find the uncertainties associated with the choices of renormalization scale and scheme significantly reduced compared to the leading-order result. We include the full dependence on the charm-quark mass m_c without any approximations. Using hadronic matrix elements estimated in the literature with lattice QCD we obtain $\tau(B^+)/\tau(B_d^0) = 1.053 \pm 0.016 \pm 0.017$, where the effects of unquenching and $1/m_b$ corrections are not yet included. The lifetime difference of heavy baryons Ξ_b^0 and Ξ_b^- is also briefly discussed.

PACS numbers: 12.38.Bx, 13.25.Hw, 14.40.Nd

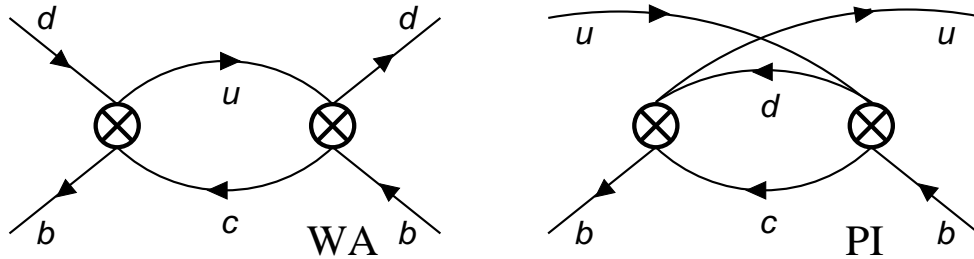


Figure 1: *Weak annihilation* (WA) and *Pauli interference* (PI) diagrams in the leading order of QCD. They contribute to $\Gamma(B_d^0)$ and $\Gamma(B^+)$, respectively. The crosses represent $|\Delta B| = 1$ operators, which are generated by the exchange of W bosons. CKM-suppressed contributions are not shown.

1 Preliminaries

The *Heavy Quark Expansion* (HQE) technique provides a well-defined QCD-based framework for the calculation of total decay rates of b -flavoured hadrons [1]. The HQE yields an expansion of the decay rate $\Gamma(H_b)$ in terms of Λ_{QCD}/m_b , where H_b represents any hadron containing a single b -quark and any of the light u, d, s (anti-)quarks as valence quarks. m_b is the b -quark mass and Λ_{QCD} is the fundamental scale of QCD, which determines the size of hadronic effects. In the leading order of Λ_{QCD}/m_b the decay rate of H_b equals the decay rate of a free b -quark, which is unaffected by the light degrees of freedom of H_b . Consequently, the lifetimes of all b -flavoured hadrons are the same at this order. The first corrections to the free quark decay appear at order $(\Lambda_{QCD}/m_b)^2$ and are caused by the Fermi motion of the b -quark in H_b and the chromomagnetic interaction of the final state quarks with the hadronic cloud surrounding the heavy b -quark. These mechanisms have a negligible effect on the lifetime difference between the B^+ and B_d^0 mesons, because the strong interaction excellently respects isospin symmetry. At order $(\Lambda_{QCD}/m_b)^3$, however, one encounters weak interaction effects between the b -quark and the light valence quark. These effects, known as *weak annihilation* (WA) and *Pauli interference* (PI) [1], are depicted in Fig. 1. They are phase-space enhanced with respect to the leading free-quark decay and induce corrections to $\Gamma(H_b)$ of order $16\pi^2(\Lambda_{QCD}/m_b)^3 = \mathcal{O}(5-10\%)$. The measurement of lifetime differences among different b -flavoured hadrons therefore tests the HQE formalism at the third order in the expansion parameter.

The calculation of $\Gamma(H_b)$ consists of three steps: the first step is an operator product expansion (OPE) integrating out the heavy W boson, which mediates the weak b decay. This results in an effective $|\Delta B| = 1$ Hamiltonian describing the flavour-changing weak interaction of the Standard Model up to corrections of order m_b^2/M_W^2 , where ΔB denotes the change in bottom-quark number:

$$H = \frac{G_F}{\sqrt{2}} V_{cb}^* \sum_{\substack{d'=d,s \\ u'=u,c}} V_{u'd'} [C_1(\mu_1) Q_1^{u'd'}(\mu_1) + C_2(\mu_1) Q_2^{u'd'}(\mu_1)] + \text{h.c.} \quad (1)$$

Here G_F is the Fermi constant and the V_{ij} 's are elements of the Cabibbo-Kobayashi-Maskawa

(CKM) matrix. The Wilson coefficients $C_i(\mu_1)$ contain the short-distance physics associated with scales above the renormalization scale μ_1 . The weak interaction is encoded in the four-quark operators

$$Q_1^{u'd'} = \bar{b}_i \gamma_\mu (1 - \gamma_5) c_j \bar{u}'_j \gamma^\mu (1 - \gamma_5) d'_i, \quad Q_2^{u'd'} = \bar{b}_i \gamma_\mu (1 - \gamma_5) c_i \bar{u}'_j \gamma^\mu (1 - \gamma_5) d'_j, \quad (2)$$

with summation over the colour indices i and j . We have omitted penguin operators and doubly Cabibbo-suppressed terms in (1), which have a negligible effect on the $B^+ - B_d^0$ lifetime difference. Next the total decay rate $\Gamma(H_b)$ is related to H by the optical theorem:

$$\Gamma(H_b) = \frac{1}{2M_{H_b}} \langle H_b | \mathcal{T} | H_b \rangle. \quad (3)$$

Here we have adopted the conventional relativistic normalization $\langle H_b | H_b \rangle = 2EV$ and introduced the transition operator:

$$\mathcal{T} = \text{Im} i \int d^4x T[H(x) H(0)]. \quad (4)$$

The second step is the HQE, which exploits the hierarchy $m_b \gg \Lambda_{QCD}$ to expand the RHS of (3) in terms of Λ_{QCD}/m_b . To this end an OPE is applied to \mathcal{T} which effectively integrates out the hard loop momenta (corresponding to the momenta of the final state quarks). We decompose the result as

$$\begin{aligned} \mathcal{T} &= [\mathcal{T}_0 + \mathcal{T}_2 + \mathcal{T}_3] [1 + \mathcal{O}(1/m_b^4)] \\ \mathcal{T}_3 &= \mathcal{T}^u + \mathcal{T}^d + \mathcal{T}_{sing} \end{aligned} \quad (5)$$

Here \mathcal{T}_n denotes the portion of \mathcal{T} which is suppressed by a factor of $1/m_b^n$ with respect to \mathcal{T}_0 describing the free quark decay. The contributions to \mathcal{T}_3 from weak spectator interactions read

$$\begin{aligned} \mathcal{T}^u &= \frac{G_F^2 m_b^2 |V_{cb}|^2}{6\pi} \left[|V_{ud}|^2 (F^u Q^d + F_S^u Q_S^d + G^u T^d + G_S^u T_S^d) \right. \\ &\quad \left. + |V_{cd}|^2 (F^c Q^d + F_S^c Q_S^d + G^c T^d + G_S^c T_S^d) \right] + (d \rightarrow s) \\ \mathcal{T}^d &= \frac{G_F^2 m_b^2 |V_{cb}|^2}{6\pi} [F^d Q^u + F_S^d Q_S^u + G^d T^u + G_S^d T_S^u]. \end{aligned} \quad (6)$$

The superscript q of the coefficients F^q , F_S^q , G^q , G_S^q refers to the cq intermediate state (see Fig. 1). We include singly Cabibbo-suppressed contributions. In writing \mathcal{T}^d we have used $|V_{ud}|^2 + |V_{us}|^2 \approx 1$ and $m_d \approx m_s \approx 0$, so that $F^d = F^s$, etc.. Here we encounter the local dimension-6, $\Delta B = 0$ operators

$$\begin{aligned} Q^q &= \bar{b} \gamma_\mu (1 - \gamma_5) q \bar{q} \gamma^\mu (1 - \gamma_5) b, & Q_S^q &= \bar{b} (1 - \gamma_5) q \bar{q} (1 + \gamma_5) b, \\ T^q &= \bar{b} \gamma_\mu (1 - \gamma_5) T^a q \bar{q} \gamma^\mu (1 - \gamma_5) T^a b, & T_S^q &= \bar{b} (1 - \gamma_5) T^a q \bar{q} (1 + \gamma_5) T^a b, \end{aligned} \quad (7)$$

where T^a is the generator of colour SU(3). We define the $\Delta B = 0$ operators at the renormalization scale μ_0 , which is of order m_b . The Wilson coefficients $F^u \dots G_S^d$ are computed in perturbation theory. When applied to mesons, \mathcal{T}^u and \mathcal{T}^d correspond to the WA and PI mechanisms of Fig. 1, respectively. In the case of baryons their role is interchanged: \mathcal{T}^u encodes the PI effect and \mathcal{T}^d describes the weak scattering of the b -quark with the valence quark (see Fig. 5). The coefficients in (6) depend on μ_0 . Since the hard loops involve the charm quark, they also depend on the ratio $z = m_c^2/m_b^2$. The truncation of the perturbation series makes $F^u \dots G_S^d$ also dependent on $\mu_1 = \mathcal{O}(m_b)$. This dependence diminishes in increasing orders of α_s . To the considered order, the dependence on μ_0 cancels between the coefficients and the matrix elements of operators in (6), so that observables are independent of μ_0 . The remainder \mathcal{T}_{sing} in (5) involves additional dimension-6 operators, which describe power-suppressed contributions to the free quark decay from strong interactions with the spectator quark. The operators in \mathcal{T}_{sing} are isospin singlets and do not contribute to the $B^+ - B_d^0$ lifetime difference. The formalism of (5)–(7) applies to weakly decaying hadrons containing a single bottom quark and no charm quarks. Decays of hadrons like the B_c meson with more than one heavy quark have a different power counting than in (5) [2]. In the third step one computes the hadronic matrix elements of the operators in (7). They enter our calculation in isospin-breaking combinations and are conventionally parametrized as [3]

$$\begin{aligned} \langle B^+ | (Q^u - Q^d)(\mu_0) | B^+ \rangle &= f_B^2 M_B^2 B_1(\mu_0), & \langle B^+ | (Q_S^u - Q_S^d)(\mu_0) | B^+ \rangle &= f_B^2 M_B^2 B_2(\mu_0), \\ \langle B^+ | (T^u - T^d)(\mu_0) | B^+ \rangle &= f_B^2 M_B^2 \epsilon_1(\mu_0), & \langle B^+ | (T_S^u - T_S^d)(\mu_0) | B^+ \rangle &= f_B^2 M_B^2 \epsilon_2(\mu_0). \end{aligned} \quad (8)$$

Here f_B is the B meson decay constant. In the *vacuum saturation approximation* (VSA) one has $B_1(\mu_0) = 1$, $B_2(\mu_0) = 1 + \mathcal{O}(\alpha_s(m_b), \Lambda_{QCD}/m_b)$ and $\epsilon_{1,2}(\mu_0) = 0$. Corrections to the VSA results are of order $1/N_c$, where $N_c = 3$ is the number of colours.

Using the isospin relation $\langle B_d^0 | Q^{d,u} | B_d^0 \rangle = \langle B^+ | Q^{u,d} | B^+ \rangle$ we now find from (3) and (6):

$$\Gamma(B_d^0) - \Gamma(B^+) = \frac{G_F^2 m_b^2 |V_{cb}|^2}{12\pi} f_B^2 M_B \left(|V_{ud}|^2 \vec{F}^u + |V_{cd}|^2 \vec{F}^c - \vec{F}^d \right) \cdot \vec{B}. \quad (9)$$

Here we have introduced the shorthand notation

$$\vec{F}^q(z, \mu_0) = \begin{pmatrix} F^q(z, \mu_0) \\ F_S^q(z, \mu_0) \\ G^q(z, \mu_0) \\ G_S^q(z, \mu_0) \end{pmatrix}, \quad \vec{B}(\mu_0) = \begin{pmatrix} B_1(\mu_0) \\ B_2(\mu_0) \\ \epsilon_1(\mu_0) \\ \epsilon_2(\mu_0) \end{pmatrix} \quad \text{for } q = d, u, c. \quad (10)$$

The strong interaction affects all three steps of the calculation. The minimal way to include QCD effects is the leading logarithmic approximation, which includes corrections of order $\alpha_s^n \ln^n(\mu_1/M_W)$, $n = 0, 1, \dots$ in the coefficients $C_{1,2}(\mu_1)$ in (1). The corresponding leading order (LO) calculation of the width difference in (9) involves the diagrams in Fig. 1 [1, 3]. Yet LO results are too crude for a precise calculation of lifetime differences. The heavy-quark masses in (9) cannot be defined in a proper way and one faces a large dependence on the renormalization scale μ_1 . Furthermore, results for $B_{1,2}$ and $\epsilon_{1,2}$ from lattice gauge theory cannot be matched to the continuum theory in a meaningful way at LO. Finally, as pointed out in [3], at LO the coefficients F , F_S in (9) are anomalously small. They multiply the large matrix elements parametrized by

$B_{1,2}$, while the larger coefficients G, G_S come with the small hadronic parameters $\epsilon_{1,2}$, rendering the LO prediction highly unstable. To cure these problems one must include the next-to-leading-order (NLO) QCD corrections of order $\alpha_s^{n+1} \ln^n(\mu_1/M_W)$. NLO corrections to the effective $|\Delta B| = 1$ Hamiltonian in (1) have been computed in [4, 5]. The second step beyond the LO requires the calculation of QCD corrections to the coefficients $F^u \dots G_S^d$ in (6). Such a calculation has been first performed for the $B_s^0 - B_d^0$ lifetime difference in [6], where $\mathcal{O}(\alpha_s)$ corrections were calculated in the $SU(3)_F$ limit neglecting certain terms of order z . In this limit only a few penguin effects play a role. A complete NLO computation has been carried out for the lifetime difference between the two mass eigenstates of the B_s^0 meson in [7]. In particular the correct treatment of infrared effects, which appear at intermediate steps of the calculation, has been worked out in [7]. The computation presented in this paper is conceptually similar to the one in [7], except that the considered transition is $\Delta B = 0$ rather than $\Delta B = 2$ and the quark masses in the final state are different. While this work was in preparation, QCD corrections to \mathcal{T}^u and \mathcal{T}^d have also been calculated in [8]. There are two important differences between our analysis and [8]:

- (i) in [8] the NLO corrections have been computed for the limiting case $z = 0$, i.e. neglecting the charm-quark mass in the final state. The corrections to this limit are of order $z \ln z$ or roughly 20%. In Sect. 2 we include the dependence on the charm-quark mass exactly.
- (ii) in [8] the $\Delta B = 0$ operators have been defined in the heavy quark effective theory (HQET) rather than in full QCD, as we did in (7). HQET operators were chosen to eliminate the mixing of the dimension-6 operators in (7) into lower-dimensional operators under renormalization. We emphasize that this mixing does not impede the use of QCD operators in the HQE: it results purely from ultraviolet effects and can be accounted for by a finite renormalization of the affected operators. For a more detailed discussion with an explicit example we refer the reader to [7] and to Sect. 3.2.

Finally one must compute the non-perturbative QCD effects residing in $f_B^2 B_1, \dots, f_B^2 \epsilon_2$. Results from lattice gauge theory for the matrix elements in (8) have been recently obtained in [9]. Earlier results using HQET fields can be found in [10]. In the matching of the results to continuum QCD the dependence of B_1, \dots, ϵ_2 on μ_0 and on the chosen renormalization scheme must cancel the corresponding dependence of the Wilson coefficients, which requires NLO accuracy.

2 \mathcal{T}^u and \mathcal{T}^d at next-to-leading order

We decompose the Wilson coefficients in (6) as

$$\begin{aligned}
 F^u(z, \mu_0) &= C_1^2(\mu_1) F_{11}^u(z, x_{\mu_1}, x_{\mu_0}) + C_1(\mu_1) C_2(\mu_1) F_{12}^u(z, x_{\mu_1}, x_{\mu_0}) \\
 &\quad + C_2^2(\mu_1) F_{22}^u(z, x_{\mu_1}, x_{\mu_0}) \\
 F_{ij}^u(z, x_{\mu_1}, x_{\mu_0}) &= F_{ij}^{u,(0)}(z) + \frac{\alpha_s(\mu_1)}{4\pi} F_{ij}^{u,(1)}(z, x_{\mu_1}, x_{\mu_0}) + \mathcal{O}(\alpha_s^2)
 \end{aligned} \tag{11}$$

with $x_\mu = \mu/m_b$ and an analogous notation for the remaining Wilson coefficients in (6). The LO coefficients are obtained from the diagrams in Fig. 1. The non-vanishing coefficients read [3]

$$\begin{aligned}
\frac{1}{3}F_{11}^{u,(0)}(z) &= \frac{1}{2}F_{12}^{u,(0)}(z) = 3F_{22}^{u,(0)}(z) = \frac{1}{2}G_{22}^{u,(0)}(z) = -(1-z)^2 \left(1 + \frac{z}{2}\right), \\
\frac{1}{3}F_{S,11}^{u,(0)}(z) &= \frac{1}{2}F_{S,12}^{u,(0)}(z) = 3F_{S,22}^{u,(0)}(z) = \frac{1}{2}G_{S,22}^{u,(0)}(z) = (1-z)^2 (1+2z), \\
\frac{1}{3}F_{11}^{c,(0)}(z) &= \frac{1}{2}F_{12}^{c,(0)}(z) = 3F_{22}^{c,(0)}(z) = \frac{1}{2}G_{22}^{c,(0)}(z) = -\sqrt{1-4z} (1-z), \\
\frac{1}{3}F_{S,11}^{c,(0)}(z) &= \frac{1}{2}F_{S,12}^{c,(0)}(z) = 3F_{S,22}^{c,(0)}(z) = \frac{1}{2}G_{S,22}^{c,(0)}(z) = \sqrt{1-4z} (1+2z), \\
6F_{11}^{d,(0)}(z) &= F_{12}^{d,(0)}(z) = 6F_{22}^{d,(0)}(z) = G_{11}^{d,(0)}(z) = G_{22}^{d,(0)}(z) = 6(1-z)^2,
\end{aligned} \tag{12}$$

while

$$\begin{aligned}
G_{11}^{u,(0)} &= G_{12}^{u,(0)} = G_{S,11}^{u,(0)} = G_{S,12}^{u,(0)} = G_{11}^{c,(0)} = G_{12}^{c,(0)} = G_{S,11}^{c,(0)} = G_{S,12}^{c,(0)} = G_{12}^{d,(0)} = 0, \\
F_{S,ij}^{d,(0)} &= G_{S,ij}^{d,(0)} = 0.
\end{aligned} \tag{13}$$

To obtain the NLO corrections $F_{ij}^{u,(1)} \dots G_{S,ij}^{d,(1)}$ we have calculated the diagrams E_i and the imaginary parts of D_i in Fig. 2. At NLO one becomes sensitive to the renormalization scheme. First, this affects the quantities m_b , z and α_s entering our calculation. The NLO coefficients given below correspond to the use of the pole-mass definition for m_b and the definition of α_s in the $\overline{\text{MS}}$ scheme [11]. z can be either calculated from the pole masses or from the $\overline{\text{MS}}$ masses, because $z = m_c^2/m_b^2 = \overline{m}_c^2(m_c)/\overline{m}_b^2(m_b) + \mathcal{O}(\alpha_s^2)$. Second, the choice of the renormalization scheme is also an issue for the effective four-quark operators appearing at the various stages of our calculation. In the prediction of physical quantities this scheme dependence cancels to the calculated order, nevertheless it must be taken care of when assembling pieces from different theoretical sources. The Wilson coefficients $C_{1,2}$ of H in (1) and $F_{ij}^{u,(1)} \dots G_{S,ij}^{d,(1)}$ depend on the scheme used to renormalize the $\Delta B = 1$ operators in (2), but this dependence cancels in $F^{u,(1)} \dots G_S^{d,(1)}$. Our results below correspond to the definition of $C_{1,2}$ in [5]. $F^{u,(1)} \dots G_S^{d,(1)}$ also depend on the renormalization scheme of the $\Delta B = 0$ operators in (7). This dependence cancels only when these coefficients are combined with the hadronic parameters $B_{1,2}$ and $\epsilon_{1,2}$ calculated from lattice QCD. It is therefore important that our scheme is used in the lattice-continuum matching of these quantities. We use the $\overline{\text{MS}}$ scheme with the NDR prescription for γ_5 [5]. To specify the scheme completely, it is further necessary to state the definition of the evanescent operators appearing in the calculation [12]. We use

$$\begin{aligned}
E[Q] &= \bar{b}\gamma_\mu\gamma_\rho\gamma_\nu(1-\gamma_5)q\bar{q}\gamma^\nu\gamma^\rho\gamma^\mu(1-\gamma_5)b - (4-8\varepsilon)Q \\
E[Q_S] &= \bar{b}\gamma_\mu\gamma_\nu(1-\gamma_5)q\bar{q}\gamma^\nu\gamma^\mu(1+\gamma_5)b - (4-8\varepsilon)Q_S
\end{aligned} \tag{14}$$

and analogous definitions of $E[T]$ and $E[T_S]$. When the diagrams $E_1 \dots E_4$ for e.g. Q_S are calculated in $D = 4 - 2\varepsilon$ dimensions, the result can be expressed as a linear combination of Q_S and $E[Q_S]$. Effectively, (14) defines how Dirac strings with two or three Dirac matrices are

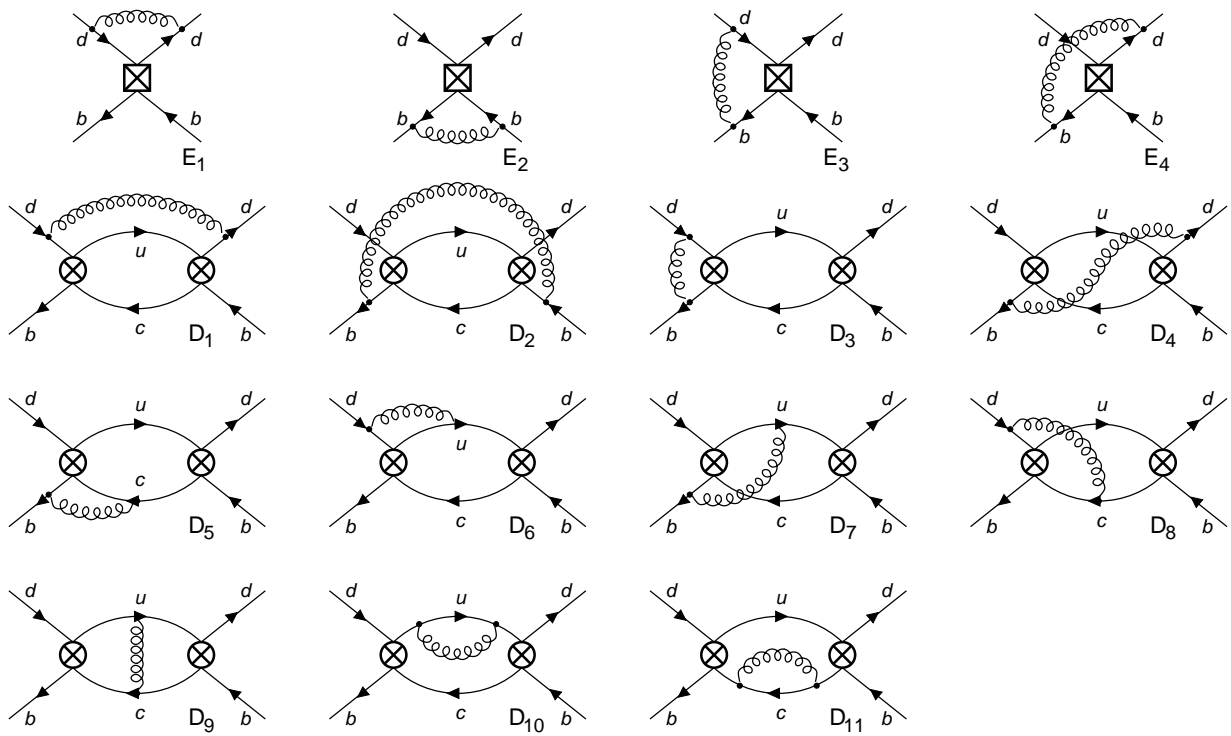


Figure 2: WA contributions in the next-to-leading order of QCD. The PI diagrams are obtained by interchanging u and d and reversing the fermion flow of the u and d lines. The first line shows the radiative corrections to $\Delta B = 0$ operators, which are necessary for the proper infrared factorization. Not displayed are the diagrams E'_3 , E'_4 and D'_{3-8} which are obtained from the corresponding unprimed diagrams by left-right reflection and the reverse of the fermion flow.

reduced. (Note that (14) also implies the replacement rules $\gamma_\nu \gamma_\rho \gamma_\mu (1 - \gamma_5) \otimes \gamma^\nu \gamma^\rho \gamma^\mu (1 - \gamma_5) \rightarrow (16 - 4\varepsilon) \gamma_\mu (1 - \gamma_5) \otimes \gamma^\mu (1 - \gamma_5)$ and $\gamma_\mu \gamma_\nu (1 - \gamma_5) \otimes \gamma^\mu \gamma^\nu (1 + \gamma_5) \rightarrow 4(1 + \varepsilon)(1 - \gamma_5) \otimes (1 + \gamma_5)$.) The particular choice of the -8ε terms in (14) is motivated by Fierz invariance: the one-loop matrix elements of e.g. Q_S and its Fierz transform $Q_S^F = -1/2 \bar{b}_i \gamma_\nu (1 + \gamma_5) b_j \bar{q}_j \gamma^\nu (1 - \gamma_5) q_i$ are in general different. This feature is an artifact of dimensional regularization. With (14) and a corresponding definition of $E[Q_S^F]$, however, Fierz invariance is maintained at the one-loop level. This choice, which has also been made in [5] for the $\Delta B = 1$ operators, has the practical advantage that one can freely use the Fierz transformation at any step of the calculation. In other words: “Fierz-evanescent” operators like $Q_S - Q_S^F$ can be identified with 0.

In the procedure of matching the full theory (eq. (4)) to the effective $\Delta B = 0$ theory, infrared singularities are encountered at $\mathcal{O}(\alpha_s)$ both in the full-theory diagrams and in the matrix elements of operators in the effective theory. The diagrams relevant for this issue are $D_1 - D_4$ and $E_1 - E_4$. The singularities cancel in the Wilson coefficients F and G , but need to be regularized at intermediate steps of the calculation. We take the b -quark on-shell, assign zero 4-momentum to the external light quarks and use dimensional regularization for the infrared (as well as the ultraviolet) divergences. In this case, care has to be taken to treat the Dirac algebra in a consistent way.

In computing the matching condition between $D_1 - D_4$ and $E_1 - E_4$ we have used two different methods, which lead to the same result. In both methods ultraviolet divergences appearing in $E_1 - E_4$ and D_3 are subtracted, respectively, by $\Delta B = 0$ and $\Delta B = 1$ counterterms, in the usual way.

In the first method, we distinguish IR singularities arising in loop integrals from UV singularities, and treat the Dirac algebra in strictly four dimensions in the IR-divergent parts. In the second method, IR and UV divergences are not distinguished and d -dimensional Dirac algebra is used throughout. In this case evanescent operators E , as those given in (14), give a non-vanishing contribution in the matching procedure. This is a subtlety of the IR regulator used in method 2 [13]. If a different IR regulator, such as a gluon mass or method 1, is used, the non-vanishing bare one-loop matrix element of E is cancelled by a finite counterterm, so that E disappears from the NLO matching calculation [5, 12]. The non-zero contribution in method 2 originates in diagram E_1 with the insertion of an evanescent operator E . This diagram is zero in dimensional regularization, thus leaving the corresponding counterterm uncanceled. We have further parametrized the evanescent $\mathcal{O}(\varepsilon)$ parts appearing in the d -dimensional projections of general Dirac structures $\Gamma \otimes \Gamma$ onto the basic operators Q and Q_S . There are four independent parameters in the calculation, corresponding to Γ being a string of two, three, four or five Dirac matrices. We have checked that all four parameters disappear from the final result for the coefficients. (This is true for the evanescent $\mathcal{O}(\varepsilon)$ parts multiplying IR poles. The UV poles give rise to a dependence on these parameters, which corresponds to a usual scheme dependence that is cancelled by the matrix elements of operators in the effective theory. Our choice of scheme is specified by (14).)

We would also like to mention that the Fierz ordering of $\Delta B = 1$ operators is immaterial because Fierz symmetry is respected by the standard NDR renormalization scheme employed by us. This has been checked by using the Fierz form leading to Dirac strings with flavour structure $\bar{b}b \otimes \bar{u}u$ in method 1, and $\bar{b}u \otimes \bar{u}b$ in method 2, and similarly for the contribution with $u \rightarrow d$. (The Fierz form used in method 2 for $\bar{b}d \otimes \bar{d}b$ is such that a closed fermion loop is generated in $D_1 - D_4$.)

In the NLO corrections to (9) we set $|V_{ud}| = 1$ and $V_{cd} = 0$. This introduces an error of order $|V_{cd}|^2 \alpha_s(m_b) z \ln z$, which is well below 1% of $\tau(B^+)/\tau(B_d^0) - 1$. Hence (9) only involves the differences $F_{ij}^{u,(1)} - F_{ij}^{d,(1)} \dots G_{S,ij}^{u,(1)} - G_{S,ij}^{d,(1)}$. Our results for these coefficients read:

$$\begin{aligned}
& F_{11}^{u,(1)}(z, x_{\mu_1}, x_{\mu_0}) - F_{11}^{d,(1)}(z, x_{\mu_1}, x_{\mu_0}) = \\
& \left[\frac{16(1-z)(-4-3z+3z^2)}{3} \right] \left[\text{Li}_2(z) + \frac{\ln(1-z)\ln(z)}{2} \right] + \\
& \left[\frac{4(1-z)^2(16+19z)}{3} \right] \ln(1-z) + \left[\frac{4z(93+40z-57z^2)}{9} \right] \ln(z) + \\
& \left[32(1-z)^2 \right] \ln(x_{\mu_1}) + \left[-16(1-z)^2 \right] \ln(x_{\mu_0}) + \\
& \left[\frac{32(1-z)}{9} \right] \pi^2 + \frac{2(1-z)(152+149z+155z^2)}{27}
\end{aligned}$$

$$\begin{aligned}
F_{12}^{u,(1)}(z, x_{\mu_1}, x_{\mu_0}) - F_{12}^{d,(1)}(z, x_{\mu_1}, x_{\mu_0}) = & \\
& \left[\frac{32(1-z)(-4-6z+z^2)}{3} \right] \left[\text{Li}_2(z) + \frac{\ln(1-z)\ln(z)}{2} \right] + \\
& \left[\frac{8(1-z)^2(2+13z+3z^2)}{3z} \right] \ln(1-z) + \left[\frac{8z(37-6z-6z^2)}{3} \right] \ln(z) + \\
& \left[16(1-z)^2(2+z) \right] \ln(x_{\mu_1}) + \left[\frac{16(1-z)(6+2z+z^2)}{9} \right] \pi^2 + \\
& \frac{4(1-z)(30+33z-13z^2)}{3}
\end{aligned}$$

$$\begin{aligned}
F_{22}^{u,(1)}(z, x_{\mu_1}, x_{\mu_0}) - F_{22}^{d,(1)}(z, x_{\mu_1}, x_{\mu_0}) = & \\
& \left[\frac{16(19-z)(-1+z)z}{9} \right] \left[\text{Li}_2(z) + \frac{\ln(1-z)\ln(z)}{2} \right] + \\
& \left[\frac{16(1-z)^2(1+2z)^2}{9z} \right] \ln(1-z) + \left[\frac{4z(135+30z-68z^2)}{27} \right] \ln(z) + \\
& \left[\frac{16(1-z)^2(8+z)}{3} \right] \ln(x_{\mu_1}) + \left[\frac{-8(1-z)^2(8+z)}{3} \right] \ln(x_{\mu_0}) + \\
& \left[\frac{16(1-z)(6+2z+z^2)}{27} \right] \pi^2 + \frac{4(1-z)(544-185z-68z^2)}{81}
\end{aligned}$$

$$\begin{aligned}
F_{S,11}^{u,(1)}(z, x_{\mu_1}, x_{\mu_0}) - F_{S,11}^{d,(1)}(z, x_{\mu_1}, x_{\mu_0}) = & \\
& \left[32(1-z)^2(1+2z) \right] \left[\text{Li}_2(z) + \frac{\ln(1-z)\ln(z)}{2} \right] + \\
& \left[-8(1-z)^2(2+10z-3z^2) \right] \ln(1-z) + \\
& \left[\frac{8z(18-155z+144z^2-27z^3)}{9} \right] \ln(z) + \\
& \left[-48(1-z)^2(1+2z) \right] \ln(x_{\mu_0}) + \frac{-4(1-z)(133-53z+40z^2)}{27}
\end{aligned}$$

$$F_{S,12}^{u,(1)}(z, x_{\mu_1}, x_{\mu_0}) - F_{S,12}^{d,(1)}(z, x_{\mu_1}, x_{\mu_0}) =$$

$$\begin{aligned}
& \left[\frac{64 (1-z) (2-z) (1+2z)}{3} \right] \left[\text{Li}_2(z) + \frac{\ln(1-z) \ln(z)}{2} \right] + \\
& \left[\frac{-16 (1-z)^2 (1+2z+6z^2-3z^3)}{3z} \right] \ln(1-z) + \\
& \left[\frac{16z (4-24z+18z^2-3z^3)}{3} \right] \ln(z) + \\
& \left[-32 (1-z)^2 (1+2z) \right] \ln(x_{\mu_1}) + \left[-32 (1-z)^2 (1+2z) \right] \ln(x_{\mu_0}) + \\
& \left[\frac{-32 (1-z) z (1+2z)}{9} \right] \pi^2 + \frac{8 (1-z) (-17-29z+36z^2)}{3}
\end{aligned}$$

$$\begin{aligned}
F_{S,22}^{u,(1)}(z, x_{\mu_1}, x_{\mu_0}) - F_{S,22}^{d,(1)}(z, x_{\mu_1}, x_{\mu_0}) = \\
& \left[\frac{32 (1-z) (3-z) (1+2z)}{9} \right] \left[\text{Li}_2(z) + \frac{\ln(1-z) \ln(z)}{2} \right] + \\
& \left[\frac{-8 (1-z)^2 (2+5z+8z^2-3z^3)}{9z} \right] \ln(1-z) + \\
& \left[\frac{8z (18-123z+82z^2-9z^3)}{27} \right] \ln(z) + \\
& \left[\frac{-32 (1-z)^2 (1+2z)}{3} \right] \ln(x_{\mu_1}) + \left[\frac{-16 (1-z)^2 (1+2z)}{3} \right] \ln(x_{\mu_0}) + \\
& \left[\frac{-32 (1-z) z (1+2z)}{27} \right] \pi^2 + \frac{4 (1-z) (-259-421z+488z^2)}{81}
\end{aligned}$$

$$\begin{aligned}
G_{11}^{u,(1)}(z, x_{\mu_1}, x_{\mu_0}) - G_{11}^{d,(1)}(z, x_{\mu_1}, x_{\mu_0}) = \\
& [16 (4-3z) (1-z)] \left[\text{Li}_2(z) + \frac{\ln(1-z) \ln(z)}{2} \right] + \\
& [(1-z)^2 (122+5z)] \ln(1-z) + \left[\frac{z (384-256z-21z^2)}{3} \right] \ln(z) + \\
& [-24 (1-z)^2] \ln(x_{\mu_1}) + [-6 (1-z)^2 (4+3z)] \ln(x_{\mu_0}) + \\
& \left[\frac{4 (7-9z) (1-z)}{3} \right] \pi^2 + \frac{(1-z) (-2450+2575z+517z^2)}{18}
\end{aligned}$$

$$\begin{aligned}
G_{12}^{u,(1)}(z, x_{\mu_1}, x_{\mu_0}) - G_{12}^{d,(1)}(z, x_{\mu_1}, x_{\mu_0}) = & \\
& [8(4-13z)(1-z)] \left[\text{Li}_2(z) + \frac{\ln(1-z)\ln(z)}{2} \right] + \\
& \left[\frac{2(1-z)^2(2+3z+13z^2)}{z} \right] \ln(1-z) + \left[\frac{4z(12+24z-25z^2)}{3} \right] \ln(z) + \\
& [12(1-z)^2(14+z)] \ln(x_{\mu_1}) + [-12(1-z)^2(8+z)] \ln(x_{\mu_0}) + \\
& \left[\frac{4(1-z)(6+2z+z^2)}{3} \right] \pi^2 + \frac{(1-z)(818-667z-19z^2)}{9}
\end{aligned}$$

$$\begin{aligned}
G_{22}^{u,(1)}(z, x_{\mu_1}, x_{\mu_0}) - G_{22}^{d,(1)}(z, x_{\mu_1}, x_{\mu_0}) = & \\
& \left[\frac{-8(1-z)(36+31z+5z^2)}{3} \right] \left[\text{Li}_2(z) + \frac{\ln(1-z)\ln(z)}{2} \right] + \\
& \left[\frac{4(1-z)^2(-1+68z+5z^2)}{3z} \right] \ln(1-z) + \left[\frac{4z(162-102z-z^2)}{9} \right] \ln(z) + \\
& [-4(1-z)^2(8+z)] \ln(x_{\mu_1}) + [2(1-z)^2(8+z)] \ln(x_{\mu_0}) + \\
& \left[\frac{2(1-z)(60+77z+7z^2)}{9} \right] \pi^2 + \frac{(1-z)(-2803+2786z+725z^2)}{27}
\end{aligned}$$

$$\begin{aligned}
G_{S,11}^{u,(1)}(z, x_{\mu_1}, x_{\mu_0}) - G_{S,11}^{d,(1)}(z, x_{\mu_1}, x_{\mu_0}) = & \\
& [-18(1-z)^2(1+2z)] \ln(1-z) + \left[\frac{-44(4-3z)z^2}{3} \right] \ln(z) + \\
& \frac{4(1-z)(28+103z-164z^2)}{9}
\end{aligned}$$

$$\begin{aligned}
G_{S,12}^{u,(1)}(z, x_{\mu_1}, x_{\mu_0}) - G_{S,12}^{d,(1)}(z, x_{\mu_1}, x_{\mu_0}) = & \\
& [16(1-z)(1+2z)] \left[\text{Li}_2(z) + \frac{\ln(1-z)\ln(z)}{2} \right] + \\
& \left[\frac{-4(1-z)^2(1+z)(1+2z)}{z} \right] \ln(1-z) + \left[\frac{4z(6-51z+28z^2)}{3} \right] \ln(z) +
\end{aligned}$$

$$\begin{aligned}
& \left[-24 (1-z)^2 (1+2z) \right] \ln(x_{\mu_1}) + \left[\frac{-8 (1-z) z (1+2z)}{3} \right] \pi^2 + \\
& \frac{4 (1-z) (-53 - 80z + 82z^2)}{9} \\
G_{S,22}^{u,(1)}(z, x_{\mu_1}, x_{\mu_0}) - G_{S,22}^{d,(1)}(z, x_{\mu_1}, x_{\mu_0}) = & \\
& \left[\frac{16 (1-z) (1+2z) (3+5z)}{3} \right] \left[\text{Li}_2(z) + \frac{\ln(1-z) \ln(z)}{2} \right] + \\
& \left[\frac{-2 (1-z)^2 (-2 + 31z + 64z^2 + 3z^3)}{3z} \right] \ln(1-z) + \\
& \left[\frac{2z (36 - 336z + 62z^2 + 9z^3)}{9} \right] \ln(z) + \\
& \left[8 (1-z)^2 (1+2z) \right] \ln(x_{\mu_1}) + \left[4 (1-z)^2 (1+2z) \right] \ln(x_{\mu_0}) + \\
& \left[\frac{-4 (1-z) (1+2z) (9+7z)}{9} \right] \pi^2 + \frac{(1-z) (385 + 1519z - 3278z^2)}{27} \quad (15)
\end{aligned}$$

Here $\text{Li}_2(z) = -\int_0^z dt [\ln(1-t)]/t$ is the dilogarithm function. Any dependence on infrared regulators has cancelled from the coefficients in (15) showing that infrared effects properly factorize. As another check we have verified that the dependence on μ_1 cancels analytically to the calculated order.

For our numerical studies we choose the following range for the input parameters:

$$\alpha_s(M_Z) = 0.118 \pm 0.003, \quad m_b = 4.8 \pm 0.1 \text{ GeV}, \quad z = 0.085 \pm 0.015. \quad (16)$$

Throughout this paper we always remove $\mathcal{O}(\alpha_s^2)$ terms from the calculated coefficients. (For instance, at NLO we write a product such as $C_1^2 F^u$ as $C_{1,\text{LO}}^2 F_{\text{NLO}}^u + 2C_{1,\text{LO}} dC_1 F_{\text{LO}}^u$, where $C_{1,\text{NLO}} = C_{1,\text{LO}} + dC_1$ denotes the NLO Wilson coefficient.) In all terms we use the two-loop expression for the running coupling α_s in QCD with five flavours. Numerical values for the calculated coefficients can be found in Tab. 1. The two contributions from $(F^u - F^d)B_1 + (G^u - G^d)\epsilon_1$ and from $(F_S^u - F_S^d)B_2 + (G_S^u - G_S^d)\epsilon_2$ to $\Gamma(B_d^0) - \Gamma(B^+)$ are separately scheme-independent. Tab. 1 reveals that the former part is expected to give the dominant contribution to the desired width difference. The results also show a substantial improvement of the μ_1 -dependence in the NLO compared to LO. This dependence is plotted in Fig. 3 for the two Wilson coefficients of the important vector operators. The approximation employed in [8] setting $z = 0$ in the NLO correction is also plotted. Expectedly, the accuracy of this approximation decreases for small μ_1 , because the difference to the exact NLO result is of order $\alpha_s(\mu_1) z \ln z$. For the final result of our coefficients we estimate the μ_1 -dependence in a more conservative way: we vary μ_1 in $F^u \dots G_S^u$ and $F^d \dots G_S^d$ independently. Further the variation with z and $\alpha_s(M_Z)$ in

z	μ_1	0.085			0.070	0.100
		$m_b/2$	m_b	$2m_b$	m_b	m_b
$F^{u,\text{LO}} - F^{d,\text{LO}}$		0.865	0.270	-0.176	0.280	0.261
$F^{u,\text{NLO}} - F^{d,\text{NLO}}$		0.396	0.460	0.386	0.469	0.452
$F_S^{u,\text{LO}} - F_S^{d,\text{LO}}$		0.002	0.042	0.105	0.043	0.042
$F_S^{u,\text{NLO}} - F_S^{d,\text{NLO}}$		0.035	0.033	0.026	0.031	0.035
$G^{u,\text{LO}} - G^{d,\text{LO}}$		-9.912	-8.618	-7.848	-8.887	-8.353
$G^{u,\text{NLO}} - G^{d,\text{NLO}}$		-8.665	-8.501	-8.154	-8.718	-8.280
$G_S^{u,\text{LO}} - G_S^{d,\text{LO}}$		2.679	2.404	2.231	2.420	2.385
$G_S^{u,\text{NLO}} - G_S^{d,\text{NLO}}$		1.668	1.850	1.902	1.854	1.843

Table 1: Numerical values for the coefficients in (9) for $\alpha_s(M_Z) = 0.118$ and $\mu_0 = m_b = 4.8 \text{ GeV}$.

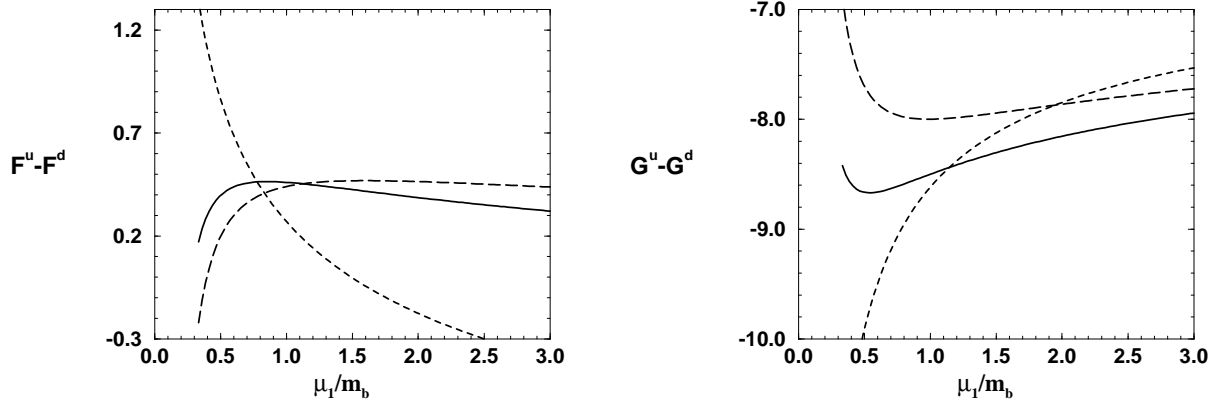


Figure 3: Dependence of $F^u - F^d$ and $G^u - G^d$ on μ_1/m_b for the input parameters in (16) and $\mu_0 = m_b$. The solid (short-dashed) line shows the NLO (LO) result. The long-dashed line shows the NLO result in the approximation of [8], i.e. z is set to zero in the NLO corrections.

the ranges of (16) is calculated and all these sources of theoretical uncertainty are symmetrized individually and added in quadrature. The dependence on z is only an issue for $G^u - G^d$. We

find:

	NLO	LO	app
$F^u - F^d$	0.460 ± 0.101	0.270 ± 0.480	0.440 ± 0.119
$F_S^u - F_S^d$	0.033 ± 0.046	0.042 ± 0.052	0.025 ± 0.045
$G^u - G^d$	-8.50 ± 0.40	-8.62 ± 0.90	-8.00 ± 0.32
$G_S^u - G_S^d$	1.85 ± 0.08	2.40 ± 0.23	1.80 ± 0.10

(17)

The quoted central values correspond to the choice $\mu_1 = m_b$ and the central values in (16). The third column in (17) shows the result for the approximation of [8], setting $z = 0$ in the NLO corrections. For $\mu_1 = m_b$ this approximation reproduces the size of the NLO corrections to $F^u - F^d$ and $G_S^u - G_S^d$ to better than 15%. The small NLO correction to $G^u - G^d$ is, however, overestimated. The NLO result for this coefficient, which is largest in magnitude, is better reproduced by the LO result than by the approximation of [8].

The origin of the $\alpha_s(\mu_1) z \ln z$ terms, which are the main cause of the discrepancy between the first and third column in (17), can be traced back to diagram D_{11} of Fig. 2. This diagram defines the scheme of the charm-quark mass. One can absorb the $\alpha_s(\mu_1) z \ln z$ terms into the LO by replacing z with $\bar{z} = \bar{m}_c^2(\mu)/\bar{m}_b^2(\mu)$, which implies the replacement

$$F^{u,(1)} \rightarrow F^{u,(1)} - \frac{\alpha_s}{4\pi} \frac{\partial F^{u,(0)}}{\partial \bar{z}} \gamma_m^{(0)} \bar{z} \ln \bar{z} \quad (18)$$

in the NLO corrections to F^u and similarly in the other Wilson coefficients. Here $\gamma_m^{(0)} = 8$ is the LO anomalous dimension of the quark mass. This procedure sums the terms of order $\alpha_s^n(\mu_1) z \ln^n z$ with $n = 0, 1, \dots$ to all orders in perturbation theory. This can be seen by performing an OPE of the transition operator \mathcal{T} which treats m_c as a light mass scale: then increasing powers of m_c correspond to $\Delta B = 0$ operators of increasing dimension and m_c and m_b enter the result at the same scale μ_1 at which the OPE is performed. In every order of the perturbation series $\ln \bar{z}$ is split into $\ln(\mu_1^2/m_b^2)$ contained in the Wilson coefficients and $\ln(m_c^2/\mu_1^2)$ residing in the matrix elements. Since there are no dimension-8 operators with charm-quark fields contributing to $\Gamma(B_d^0) - \Gamma(B^+)$, no terms of order $m_c^2 \ln(m_c^2/\mu_1^2)$ can occur. From our NLO results we can indeed verify that the procedure in (18) removes the $\alpha_s(\mu_1) z \ln z$ terms, while e.g. terms of order $\alpha_s(\mu_1) z^2 \ln z$ persist as expected, because there are dimension-10 operators with charm-quark fields of the type $m_c(\bar{b}q)(\bar{q}b)(\bar{c}c)$. Using $\bar{z} = 0.055$ rather than $z = 0.085$ in the coefficients tabulated in the third column of (17) indeed removes the disturbing discrepancy with the NLO result for $G^u - G^d$. Also the central values of $F^u - F^d$ and $G_S^u - G_S^d$ move closer to the NLO result, while no significant improvement occurs for $F_S^u - F_S^d$.

The width difference in (9) involves the product $\vec{F}^{qT} \vec{B}$, which is independent of the renormalization scheme and scales. In order to compare the scheme dependent coefficients \vec{F}^q with the calculation in [8] for $z = 0$, we need to take into account that the coefficients in [8] are defined for matrix elements in HQET rather than in full QCD. The matching relation connecting HQET and full-QCD matrix elements of the four operators \vec{O} used in [8] has the form

$$\langle \vec{O} \rangle_{QCD}(m_b) = \left(1 + \frac{\alpha_s(m_b)}{4\pi} \hat{C}_1^{\overline{MS}} \right) \langle \vec{O} \rangle_{HQET}(m_b), \quad (19)$$

where the 4×4 matrix $\hat{C}_1^{\overline{MS}}$ can be found in Eq. (36) of [8]. The renormalization scheme of operator matrix elements in full QCD is identical in our paper and in [8,9]. The only further difference is that the operators \vec{O} are linear combinations, $\vec{O} = S\vec{Q}$, of our basis $\vec{Q} = (Q, Q_S, T, T_S)^T$ with

$$S = \begin{pmatrix} \frac{1}{3} & 0 & 2 & 0 \\ 0 & -\frac{2}{3} & 0 & -4 \\ \frac{4}{9} & 0 & -\frac{1}{3} & 0 \\ 0 & -\frac{8}{9} & 0 & \frac{2}{3} \end{pmatrix}. \quad (20)$$

(This simple relation holds beyond tree level because the renormalization schemes are identical. The preservation of Fierz-symmetry by the choice of evanescent operators in (14) is important for this property.) It follows that our coefficients \vec{F} are related to the corresponding coefficients $\vec{A} + \frac{\alpha_s}{4\pi}\vec{B}$ in [8] at scale $\mu = m_b$ through

$$\frac{1}{3} \left(\vec{F}^{(0)} + \frac{\alpha_s}{4\pi} \vec{F}^{(1)} \right)^T = \vec{A}^T S + \frac{\alpha_s}{4\pi} \left(\vec{B}^T S - \vec{A}^T \hat{C}_1^{\overline{MS}} S \right). \quad (21)$$

Here we have suppressed flavour labels $q = u, d$ and the double indices $ij = 11, 12, 22$ referring to the $\Delta B = 1$ coefficients $C_i C_j$ (see (11)). Note that in the notation of [8] labels u, d are interchanged with respect to our convention and that the coefficients with label 12 are defined with a relative factor of two. Using (21) we have verified that the results of [8] obtained for $z = 0$ are in agreement with ours in this limit.

3 Phenomenology

3.1 $\tau(B^+)/\tau(B_d^0)$

One can directly use (9) to predict the desired lifetime ratio:

$$\begin{aligned} \frac{\tau(B^+)}{\tau(B_d^0)} - 1 &= \tau(B^+) \left[\Gamma(B_d^0) - \Gamma(B^+) \right] \\ &= 0.0325 \left(\frac{|V_{cb}|}{0.04} \right)^2 \left(\frac{m_b}{4.8 \text{ GeV}} \right)^2 \left(\frac{f_B}{200 \text{ MeV}} \right)^2 \times \\ &\quad \left[(1.0 \pm 0.2) B_1 + (0.1 \pm 0.1) B_2 - (18.4 \pm 0.9) \epsilon_1 + (4.0 \pm 0.2) \epsilon_2 \right]. \end{aligned} \quad (22)$$

Here $\tau(B^+) = 1.653$ ps has been used in the overall factor and the hadronic parameters $B_1 \dots \epsilon_2$ are normalized at $\mu_0 = m_b$ throughout this section.

In [3] it has been noticed that without a detailed study of the hadronic parameters one expects $\tau(B^+)/\tau(B_d^0)$ to deviate from 1 by up to $\pm 20\%$. This feature originates from the large coefficient of ϵ_1 and persists in our NLO prediction in (22), because the NLO corrections to $G^u - G^d$ are small. Confronting (22) with the recent measurements [14, 15],

$$\frac{\tau(B^+)}{\tau(B_d^0)} = \begin{cases} 1.082 \pm 0.026 \pm 0.012 & \text{(BABAR)} \\ 1.091 \pm 0.023 \pm 0.014 & \text{(BELLE)} \end{cases} \quad (23)$$

one expects $|\epsilon_1|$ to be significantly smaller than $1/N_c = 1/3$, i.e. nonfactorizable contributions appear to be small. This result is confirmed by the existing computations of the ϵ_i 's in quenched lattice QCD [9, 10]. However, due to its large coefficient sophisticated non-perturbative methods are definitely necessary to compute ϵ_1 sufficiently accurately. The other important term in (22) is the first one: the NLO enhancement of $F^u - F^d$ in (17) has altered the coefficient of B_1 in (22) from 0.6 ± 1.0 in the LO to 1.0 ± 0.2 . While from the LO result not even the sign of this contribution was known, the NLO result now clearly establishes a positive contribution of order 3% to $\tau(B^+)/\tau(B_d^0)$ from the term involving B_1 .

The hadronic parameters have been computed in [9] using the same renormalization scheme as in the present paper. They read

$$(B_1, B_2, \epsilon_1, \epsilon_2) = (1.10 \pm 0.20, 0.79 \pm 0.10, -0.02 \pm 0.02, 0.03 \pm 0.01). \quad (24)$$

Using $|V_{cb}| = 0.040 \pm 0.0016$ from a CLEO analysis of inclusive semileptonic B decays [16], the world average $f_B = (200 \pm 30)$ MeV from lattice calculations [17] and $m_b = 4.8 \pm 0.1$ GeV in (22), we find

$$\frac{\tau(B^+)}{\tau(B_d^0)} = 1.053 \pm 0.016 \pm 0.017, \quad \left[\frac{\tau(B^+)}{\tau(B_d^0)} \right]_{\text{LO}} = 1.041 \pm 0.040 \pm 0.013, \quad (25)$$

where the first error is due to the errors on the NLO coefficients as given in (22) and the hadronic parameters (24), and the second error is the overall normalization uncertainty due to m_b , $|V_{cb}|$ and f_B in (22). The first error reduces to 0.008 in NLO and 0.038 in LO, if the errors on the hadronic parameters are neglected, demonstrating the substantial reduction of scale dependence at NLO in comparison with the LO. This result is gratifying as the strong scale dependence observed at LO had been a major motivation for a NLO analysis. This is also seen in Fig. 4, where we show the lifetime ratio as a function of the renormalization scale μ_1 . We should, however, emphasize that the result and error given in (25) do not include the effects of $1/m_b$ corrections and unquenching, which could well be on the order of 0.05. The NLO result slightly exceeds the central value of the LO result and improves the agreement with the experimental value in (23).

3.2 $\tau(\Xi_b^0)/\tau(\Xi_b^-)$

The $SU(3)_F$ anti-triplet ($\Lambda_b \sim bud$, $\Xi_b^0 \sim bus$, $\Xi_b^- \sim bds$) comprises the b -flavoured baryons whose light degrees of freedom are in a 0^+ state. These baryons decay weakly. Baryon lifetimes have attracted a lot of theoretical attention: the measured Λ_b lifetime falls short of $\tau(B_d^0)$ by roughly 20% [18], which has raised concerns about the applicability of the HQE to baryons. Unfortunately this interesting topic cannot yet be addressed at the NLO level, because $\tau(\Lambda_b)/\tau(B_d^0)$ receives contributions from the $SU(3)_F$ -singlet portion \mathcal{T}_{sing} of the transition operator in (5) and NLO corrections to \mathcal{T}_{sing} are unknown at present. Further the hadronic matrix elements entering $\tau(\Lambda_b)/\tau(B_d^0)$ involve penguin contractions of the operators in (7), which are difficult to compute. It is, however, possible to predict the lifetime splitting within the iso-doublet (Ξ_b^0, Ξ_b^-) with NLO precision. The corresponding LO diagrams are shown in Fig. 5. For Ξ_b 's the weak decay of the valence s -quark could be relevant: the decays $\Xi_b^- \rightarrow \Lambda_b \pi^-$, $\Xi_b^- \rightarrow \Lambda_b e^- \bar{\nu}_e$ and $\Xi_b^0 \rightarrow \Lambda_b \pi^0$

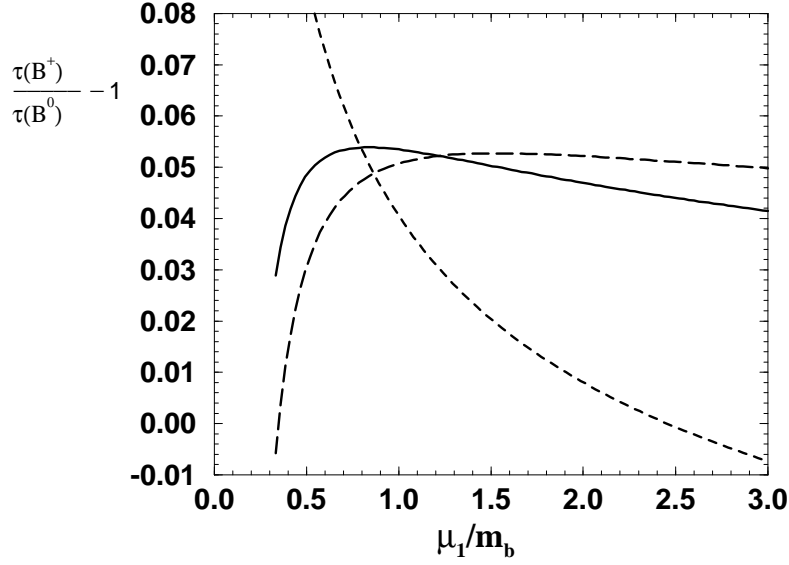


Figure 4: Dependence of $\tau(B^+)/\tau(B^0) - 1$ on μ_1/m_b for the central values of the input parameters and $\mu_0 = m_b$. The solid (short-dashed) line shows the NLO (LO) result. The long-dashed line shows the NLO result in the approximation of [8], i.e. z is set to zero in the NLO corrections.

are triggered by $s \rightarrow u$ transitions and could affect the total rates at the $\mathcal{O}(1\%)$ level [19]. Once the lifetime measurements reach this accuracy, one should correct for this effect. To this end we define

$$\bar{\Gamma}(\Xi_b) \equiv \Gamma(\Xi_b) - \Gamma(\Xi_b \rightarrow \Lambda_b X) = \frac{1 - B(\Xi_b \rightarrow \Lambda_b X)}{\tau(\Xi_b)} \equiv \frac{1}{\bar{\tau}(\Xi_b)} \quad \text{for } \Xi_b = \Xi_b^0, \Xi_b^-, \quad (26)$$

where $B(\Xi_b \rightarrow \Lambda_b X)$ is the branching ratio of the above-mentioned decay modes. Thus $\bar{\Gamma}(\Xi_b)$ is the contribution from $b \rightarrow c$ transitions to the total decay rate. In analogy to (9) one finds

$$\bar{\Gamma}(\Xi_b^-) - \bar{\Gamma}(\Xi_b^0) = \frac{G_F^2 m_b^2 |V_{cb}|^2}{12\pi} f_B^2 M_B \left(|V_{ud}|^2 \vec{F}^u + |V_{cd}|^2 \vec{F}^c - \vec{F}^d \right) \cdot \vec{B}^{\Xi_b}. \quad (27)$$

Here $\vec{B}^{\Xi_b} = (L_1^{\Xi_b}(\mu_0), L_{1S}^{\Xi_b}(\mu_0), L_2^{\Xi_b}(\mu_0), L_{2S}^{\Xi_b}(\mu_0))^T$ comprises the hadronic parameters defined as

$$\begin{aligned} \langle \Xi_b^0 | (Q^u - Q^d)(\mu_0) | \Xi_b^0 \rangle &= f_B^2 M_B M_{\Xi_b} L_1^{\Xi_b}(\mu_0), \\ \langle \Xi_b^0 | (Q_S^u - Q_S^d)(\mu_0) | \Xi_b^0 \rangle &= f_B^2 M_B M_{\Xi_b} L_{1S}^{\Xi_b}(\mu_0), \\ \langle \Xi_b^0 | (T^u - T^d)(\mu_0) | \Xi_b^0 \rangle &= f_B^2 M_B M_{\Xi_b} L_2^{\Xi_b}(\mu_0), \\ \langle \Xi_b^0 | (T_S^u - T_S^d)(\mu_0) | \Xi_b^0 \rangle &= f_B^2 M_B M_{\Xi_b} L_{2S}^{\Xi_b}(\mu_0). \end{aligned} \quad (28)$$

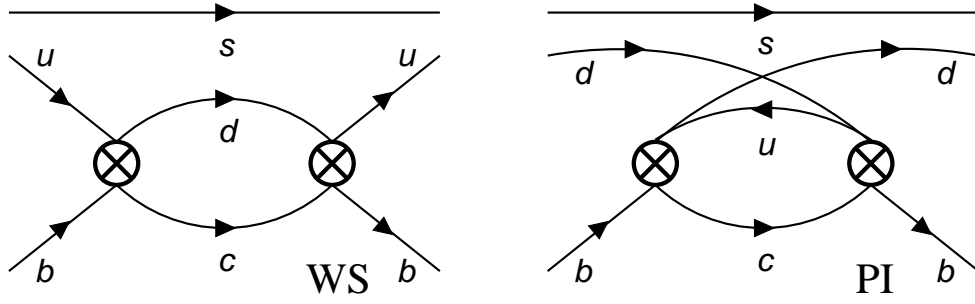


Figure 5: *Weak scattering* (WS) and *PI* diagrams for Ξ_b baryons in the leading order of QCD. They contribute to $\Gamma(\Xi_b^0)$ and $\Gamma(\Xi_b^-)$, respectively. CKM-suppressed contributions are not shown.

In contrast to the B meson system, the four matrix elements in (28) are not independent at the considered order in Λ_{QCD}/m_b . Since the light degrees of freedom are in a spin-0 state, the matrix elements $\langle \Xi_b | 2Q_S^q + Q^q | \Xi_b \rangle$ and $\langle \Xi_b | 2T_S^q + T^q | \Xi_b \rangle$ are power-suppressed compared to those in (28) (see e.g. [1, 3]). This, however, is not true in all renormalization schemes, in the $\overline{\text{MS}}$ scheme used by us $2Q_S^q + Q^q$ and $2T_S^q + T^q$ receive short-distance corrections, because hard gluons can resolve the heavy b -quark mass. This feature is discussed in [7]. These short-distance corrections are calculated from the diagrams $E_1 \dots E_4$ in Fig. 2. For our scheme we find

$$\begin{pmatrix} L_{1S}^{\Xi_b}(m_b) \\ L_{2S}^{\Xi_b}(m_b) \end{pmatrix} = \left[-\frac{1}{2} + \frac{\alpha_s(m_b)}{4\pi} \begin{pmatrix} -28/3 & -7 \\ -14/9 & 7/2 \end{pmatrix} \right] \begin{pmatrix} L_1^{\Xi_b}(m_b) \\ L_2^{\Xi_b}(m_b) \end{pmatrix} + \mathcal{O}\left(\frac{\Lambda_{QCD}}{m_b}\right). \quad (29)$$

As an important check we find that the dependence on the infrared regulator drops out in (29). With (29) we can express the width difference in (27) in terms of just the two hadronic parameters $L_1^{\Xi_b}$ and $L_2^{\Xi_b}$. We find

$$\begin{aligned} \frac{\bar{\tau}(\Xi_b^0)}{\bar{\tau}(\Xi_b^-)} - 1 &= \bar{\tau}(\Xi_b^0) \left[\Gamma(\Xi_b^-) - \Gamma(\Xi_b^0) \right] \\ &= 0.59 \left(\frac{|V_{cb}|}{0.04} \right)^2 \left(\frac{m_b}{4.8 \text{ GeV}} \right)^2 \left(\frac{f_B}{200 \text{ MeV}} \right)^2 \frac{\bar{\tau}(\Xi_b^0)}{1.5 \text{ ps}} \times \\ &\quad \left[(0.04 \pm 0.01) L_1 - (1.00 \pm 0.04) L_2 \right], \quad (30) \end{aligned}$$

with $L_i = L_i^{\Xi_b}(\mu_0 = m_b)$. For the baryon case there is no reason to expect the color-octet matrix element to be much smaller than the color-singlet ones, so that the term with L_2 will dominate the result. The hadronic parameters $L_{1,2}$ have been analysed in an exploratory study of lattice HQET [20] for Λ_b baryons. Up to $\text{SU}(3)_F$ corrections, which are irrelevant in view of the other uncertainties, $L_i^{\Xi_b}$ and $L_i^{\Lambda_b}$ are equal.

4 Conclusions

We have computed the Wilson coefficients in the heavy quark expansion to order $(\Lambda_{QCD}/m_b)^3$ for the $B^+ - B_d^0$ lifetime difference at next-to-leading order in perturbative QCD. These coeffi-

icients depend on the scheme and scale μ_0 used to define the matrix elements of the $\Delta B = 0$ operators in the effective theory. Our scheme is specified by the NDR prescription for γ_5 , $\overline{\text{MS}}$ subtraction and the definition of evanescent operators given in (14). The $\mathcal{O}(\alpha_s)$ accuracy is crucial for a satisfactory matching of the Wilson coefficients to the matrix elements determined with lattice QCD. Current lattice calculations, which are still in a relatively early stage in this case, yield, when combined with our calculations, $\tau(B^+)/\tau(B_d^0) = 1.053 \pm 0.016 \pm 0.017$ [see (25)]. The effects of unquenching and $1/m_b$ corrections are not yet included, but could well be on the order of 0.05. Next-to-leading order corrections to $\tau(B^+)/\tau(B_d^0)$ were recently computed in the approximation $m_c = 0$ [8]. Taking the limit $m_c \rightarrow 0$ of our results we find agreement with this calculation.

A substantial improvement of the NLO calculation is the large reduction of perturbative uncertainty reflected in the scale dependence of $\Delta B = 1$ Wilson coefficients from the standard weak Hamiltonian. This scale dependence had been found to be very large at leading order, preventing even an unambiguous prediction of the sign of $\tau(B^+)/\tau(B_d^0) - 1$ up to now [3]. With this major source of uncertainty removed by the NLO calculation, further progress will depend on continuing advances in the evaluation of the nonperturbative hadronic matrix elements and the computation of $1/m_b$ -suppressed effects.

References

- [1] M. A. Shifman and M. B. Voloshin, in: *Heavy Quarks* ed. V. A. Khoze and M. A. Shifman, Sov. Phys. Usp. **26** (1983) 387; M. A. Shifman and M. B. Voloshin, Sov. J. Nucl. Phys. **41** (1985) 120 [Yad. Fiz. **41** (1985) 187]; M. A. Shifman and M. B. Voloshin, Sov. Phys. JETP **64** (1986) 698 [Zh. Eksp. Teor. Fiz. **91** (1986) 1180]; I. I. Bigi, N. G. Uraltsev and A. I. Vainshtein, Phys. Lett. B **293** (1992) 430 [Erratum-ibid. B **297** (1992) 477]. For a recent review see: M. Voloshin, in: *B physics at the Tevatron: Run-II and Beyond*, Chapter 8, [hep-ph/0201071].
- [2] M. Beneke and G. Buchalla, Phys. Rev. D **53** (1996) 4991.
- [3] M. Neubert and C. T. Sachrajda, Nucl. Phys. B **483** (1997) 339. M. Beneke, G. Buchalla and I. Dunietz, Phys. Rev. D **54** (1996) 4419.
- [4] G. Altarelli, G. Curci, G. Martinelli and S. Petrarca, Nucl. Phys. B **187** (1981) 461.
- [5] A. J. Buras and P. H. Weisz, Nucl. Phys. B **333** (1990) 66.
- [6] Y. Y. Keum and U. Nierste, Phys. Rev. D **57** (1998) 4282.
- [7] M. Beneke, G. Buchalla, C. Greub, A. Lenz and U. Nierste, Phys. Lett. B **459** (1999) 631.
- [8] M. Ciuchini, E. Franco, V. Lubicz and F. Mescia, [hep-ph/0110375].
- [9] D. Becirevic, [hep-ph/0110124].

- [10] M. Di Pierro and C. T. Sachrajda [UKQCD Collaboration], Nucl. Phys. B **534** (1998) 373; Nucl. Phys. Proc. Suppl. **73** (1999) 384.
- [11] W. A. Bardeen, A. J. Buras, D. W. Duke and T. Muta, Phys. Rev. D **18** (1978) 3998.
- [12] S. Herrlich and U. Nierste, Nucl. Phys. B **455** (1995) 39.
- [13] M. Misiak and J. Urban, Phys. Lett. B **451** (1999) 161.
- [14] B. Aubert *et al.* [BABAR Collaboration], Phys. Rev. Lett. **87** (2001) 201803.
- [15] K. Abe [Belle Collaboration], [hep-ex/0202009].
- [16] D. Cassel [CLEO coll.], talk at *Lepton Photon 01*, 23-28 Jul 2001, Rome, Italy.
- [17] S. Ryan, [hep-lat/0111010].
- [18] D. E. Groom *et al.* [Particle Data Group Collaboration], Eur. Phys. J. C **15** (2000) 1; updated at <http://pdg.lbl.gov>.
- [19] M. B. Voloshin, Phys. Lett. B **476** (2000) 297.
- [20] M. Di Pierro, C. T. Sachrajda and C. Michael [UKQCD collaboration], Phys. Lett. B **468** (1999) 143.